MLCT and LMCT Transitions in Acetylide Complexes. Structural, Spectroscopic, and Redox Properties of Ruthenium(II) and -(III) Bis(*σ*-arylacetylide) Complexes Supported by a Tetradentate Macrocyclic Tertiary Amine Ligand

Mei-Yuk Choi,[†] Michael Chi-Wang Chan,[†] Suobo Zhang,[†] Kung-Kai Cheung,[†] Chi-Ming Che,*[,†] and Kwok-Yin Wong[‡]

Department of Chemistry, The University of Hong Kong, Pokfulam Road, Hong Kong, and Department of Applied Biology and Chemical Technology, The Hong Kong Polytechnic University, Kowloon, Hong Kong

Received January 11, 1999

Ruthenium(II) complexes *trans*-[Ru(16-TMC)(C≡CC_6H_4X-*p*)$_2$] (X = OMe (**1**), Me (**2**), H (**3**), F (**4**), Cl (**5**); 16-TMC = 1,5,9,13-tetramethyl-1,5,9,13-tetraazacyclohexadecane) are prepared by the reaction of [Ru^{III}(16-TMC)Cl_2]Cl with the corresponding alkyne and NaOMe in the presence of zinc amalgam. Low ν(C≡C) stretching frequencies are observed for **1**−**5** and are attributed to the *σ*-donating nature of 16-TMC. The molecular structures of **1**, **3**, and **5** have been determined by X-ray crystal analyses, which reveal virtually identical Ru−C and C≡C bond distances (mean 2.076 and 1.194 Å, respectively). The cyclic voltammograms of **1**−**5** show quasi-reversible $Ru^{III/II}$ and $Ru^{IV/III}$ oxidation couples. Oxidative cleavage of the acetylide ligand in **3** by dioxygen affords [Ru(16-TMC)(C≡CPh)(CO)]$^+$ (**6**). Ruthenium(III) derivatives *trans*-[Ru(16-TMC)(C≡CC_6H_4X-*p*)$_2$]$^+$ are generated in situ by electrochemical oxidation in dichloromethane or by chemical oxidation of **1**−**5** with Ce(IV). Their UV−visible absorption spectra show a vibronically structured absorption band with λ_{max} at 716−768 nm. The vibrational progressions, which range from 1730 to 1830 cm^{-1}, imply that the electronic transition involves distortion of the acetylide ligand in the excited state. An assignment of p_π(ArC≡C) → d_{π^*}(Ru^{III}) charge transfer is proposed for this transition.

Introduction

The chemistry of *σ*-acetylide transition-metal complexes has experienced intense scrutiny.[1,2] In principle, the linear C≡C moiety allows delocalization of electron density and thus electronic communication between metal centers and remote functional groups. The nature of the metal−acetylide interaction is manifested in specific properties which are applicable to several areas of material science and fundamental research, including nonlinear optical materials,[3] liquid crystals,[4] polymeric conductors,[5] and conjugated carbon-rich chains and molecular wires.[6] Significantly, several recent reports have provided valuable insights toward a comprehensive description of the metal−acetylide bond by spectroscopic and theoretical means.[7−9] For electron-rich metal centers, M → (CCR) π back-bonding interactions with

[†] The University of Hong Kong.
[‡] The Hong Kong Polytechnic University.

(1) Nast, R. *Coord. Chem. Rev.* **1982**, *47*, 89.
(2) Manna, J.; John, K. D.; Hopkins, M. D. *Adv. Organomet. Chem.* **1995**, *38*, 79.
(3) (a) Nguyen, P.; Lesley, G.; Marder, T. B.; Ledoux, I.; Zyss, J. *Chem. Mater.* **1997**, *9*, 406. (b) Whittall, I. R.; Humphrey, M. G.; Samoc, M.; Luther-Davies, B. *Angew. Chem., Int. Ed. Engl.* **1997**, *36*, 370. (c) McDonagh, A. M.; Whittall, I. R.; Humphrey, M. G.; Hockless, D. C. R.; Skelton, B. W.; White, A. H. *J. Organomet. Chem.* **1996**, *523*, 33. (d) Houbrechts, S.; Clays, K.; Persoons, A.; Cadierno, V.; Gamasa, M. P.; Gimeno, J. *Organometallics* **1996**, *15*, 5266. (e) Long, N. J. *Angew. Chem., Int. Ed. Engl.* **1995**, *34*, 21. (f) Whittall, I. R.; Humphrey, M. G.; Hockless, D. C. R.; Skelton, B. W.; White, A. H. *Organometallics* **1995**, *14*, 3970. (g) Myers, L. K.; Langhoff, C.; Thompson, M. E. *J. Am. Chem. Soc.* **1992**, *114*, 4, 7560. (h) McDonagh, A. M.; Humphrey, M. G.; Samoc, M.; Luther-Davies, B.; Houbrechts, S.; Wada, T.; Sasabe, H.; Persoons, A. *J. Am. Chem. Soc.* **1999**, *121*, 1405.
(4) (a) Takahashi, S.; Takai, Y.; Morimoto, H.; Sonogashira, K. *J. Chem. Soc., Chem. Commun.* **1984**, 3. (b) Altmann, M.; Enkelmann, V.; Lieser, G.; Bunz, U. H. F. *Adv. Mater.* **1995**, *7*, 726. (c) Altmann, M.; Bunz, U. H. F. *Angew. Chem., Int. Ed. Engl.* **1995**, *34*, 569. (d) Rourke, J. P.; Bruce, D. W.; Marder, T. B. *J. Chem. Soc., Dalton Trans.* **1995**, 317.
(5) (a) Puddephatt, R. J. *Chem. Commun.* **1998**, 1055. (b) Adams, C. J.; James, S. L.; Raithby, P. R. *Chem. Commun.* **1997**, 2155. (c) Manners, I. *Angew. Chem., Int. Ed. Engl.* **1996**, *35*, 1602. (d) Markwell, R. D.; Butler, I. S.; Kakkar, A. K.; Khan, M. S.; Al-Zakwani, Z. H.; Lewis, J. *Organometallics* **1996**, *15*, 2331. (e) Frapper, G.; Kertesz, M. *Inorg. Chem.* **1993**, *32*, 732.
(6) (a) Leininger, S.; Stang, P. J.; Huang, S. *Organometallics* **1998**, *17*, 3981. (b) Uno, M.; Dixneuf, P. H. *Angew. Chem., Int. Ed.* **1998**, *37*, 1714. (c) Brady, M.; Weng, W.; Zhou, Y.; Seyler, J. W.; Amoroso, A. J.; Arif, A. M.; Böhme, M.; Frenking, G.; Gladysz, J. A. *J. Am. Chem. Soc.* **1997**, *119*, 775. (d) Lavastre, O.; Plass, J.; Bachmann, P.; Guesmi, S.; Moinet, C.; Dixneuf, P. H. *Organometallics* **1997**, *16*, 184. (e) Xia, H. P.; Wu, W. F.; Ng, W. S.; Williams, I. D.; Jia, G. *Organometallics* **1997**, *16*, 2940. (f) Coat, F.; Guillevic, M.-A.; Toupet, L.; Paul, F.; Lapinte, C. *Organometallics* **1997**, *16*, 5988. (g) Harriman, A.; Ziessel, R. *Chem. Commun.* **1996**, 1707. (h) Bunz, U. H. F. *Angew. Chem., Int. Ed. Engl.* **1996**, *35*, 969. (i) Bruce, M. I.; Ke, M.; Low, P. J. *Chem. Commun.* **1996**, 2405. (j) Yam, V. W. W.; Lau, V. C. Y.; Cheung, K. K. *Organometallics* **1996**, *15*, 1740. (k) Pirio, N.; Touchard, D.; Dixneuf, P. H.; Fettouhi, M.; Ouahab, L. *Angew. Chem., Int. Ed. Engl.* **1992**, *31*, 651.
(7) John, K. D.; Stoner, T. C.; Hopkins, M. D. *Organometallics* **1997**, *16*, 4948.
(8) McGrady, J. E.; Lovell, T.; Stranger, R.; Humphrey, M. G. *Organometallics* **1997**, *16*, 4004.
(9) Lichtenberger, D. L.; Renshaw, S. K.; Bullock, R. M. *J. Am. Chem. Soc.* **1993**, *115*, 3276.

10.1021/om990009d CCC: $18.00
Publication on Web 04/28/1999

electron-poor acetylide groups typically prevail and lead to delocalization of the metal dπ electrons into the acetylide π* orbital. Alternatively, π back-bonding is negligible with electron-deficient metal ions, but metal−carbon multiple-bonding interactions in the M−C≡CR linkage are possible. This would result in considerable acetylide-to-metal charge transfer, yet this observation is rarely made.

Ruthenium is an established π donor in the +2 oxidation state but is also known to form metal−ligand multiple-bonded species in oxidation states ≥4.[10] Numerous studies have appeared describing the reactivity of ruthenium σ-acetylide complexes supported by mono- and bidentate phosphine ligands.[11] Nitrogen donors have been incorporated to a lesser extent, although such endeavors can yield rewarding results.[12,13] We became interested in (σ-acetylide)ruthenium complexes of the macrocyclic tertiary amine 1,5,9,13-tetramethyl-1,5,9,-13-tetraazacyclohexadecane (16-TMC). Generation of *trans*-bis(acetylide) derivatives would facilitate linear rigid-rod applications. This tetradentate amine and its congeners (14- and 15-TMC) are optically transparent in the UV−visible spectral region, and this permits investigation of the metal-to-ligand or ligand-to-metal charge transfer (MLCT or LMCT, respectively) electronic transitions associated with the Ru−C≡CR moiety by optical spectroscopy. This class of ligands constitutes strong σ donors, is resistant to oxidation, and can accommodate reactive but isolable high-valent oxoruthenium complexes.[14,15] We envisaged that the 16-TMC ligand would maximize Ru(II) → CCR π back-bonding and stabilize organoruthenium species in high oxidation states.

We now describe the synthesis and structural and redox properties of a series of *trans*-bis(σ-arylacetylide)-ruthenium complexes, which are the first to contain a macrocyclic N-donor ligand, namely 16-TMC. Because of the optical transparency of the tertiary amine, we have been able to probe the MLCT and LMCT transitions associated with the $[Ru^{II}(C{\equiv}CAr)_2]$ and $[Ru^{III}(C{\equiv}CAr)_2]^+$ cores, respectively.

Experimental Section

All reactions were performed under a nitrogen atmosphere using standard Schlenk techniques unless otherwise stated. Solvents were purified by standard methods. All reagents were used as received. [Ru(16-TMC)Cl_2]Cl (16-TMC = 1,5,9,13-tetramethyl-1,5,9,13-tetraazacyclohexadecane) was prepared according to the published procedure.[14]

^{1}H and $^{13}C\{^1H\}$ NMR spectra were recorded on JEOL 270, Bruker 300 DPX, and Bruker 500 DRX FT-NMR spectrometers. Peak positions were calibrated with Me_4Si as internal standard. In the $^{13}C\{^1H\}$ NMR spectra, multiple resonances for 16-TMC are observed because of the flexible nature of the propylene groups, and the peaks listed correspond to the most intense signals. Fast atom bombardment (FAB) mass spectra were obtained on a Finnigan MAT 95 mass spectrometer with a 3-nitrobenzyl alcohol matrix. Infrared spectra were recorded as KBr plates on a Bio-Rad FT-IR spectrometer. Raman spectra were recorded on a Bio-Rad FT Raman spectrometer. UV−visible spectra were recorded on Perkin-Elmer Lambda 19 and Milton Roy (Spectronic 3000 Array) diode array spectrophotometers. Elemental analyses were performed by the Butterworth Laboratories Ltd., Teddington, U.K.

Cyclic voltammetry was performed with a Bioanalytical Systems (BAS) Model 100 B/W electrochemical analyzer. A conventional two-compartment electrochemical cell was used. The glassy-carbon electrode was polished with 0.05 μm alumina on a microcloth, sonicated for 5 min in deionized water, and rinsed with dichloromethane before use. An $Ag/AgNO_3$ (0.1 M in CH_3CN) electrode was used as reference electrode. All solutions were degassed with argon gas before experiments. $E_{1/2}$ values are the average of the cathodic and anodic peak potentials for the oxidative and reductive waves. The $E_{1/2}$ value of the ferrocenium/ferrocene couple ($Cp_2Fe^{+/0}$) measured in the same solution was used as an internal reference (+0.23 mV in CH_2Cl_2). Thin-layer UV−vis spectroelectrochemistry was performed by using the HP 8452A diode array spectrophotometer and Princeton Applied Research Model 273A potentiostat, a thin-layer quartz cell of path length 0.5 mm with a platinum-gauze working electrode, a platinum-wire counter electrode, and a $Ag/AgNO_3$ reference electrode.

Syntheses. *trans*-[Ru(16-TMC)(C≡CC_6H_4X-*p*)$_2$]. Sodium metal (0.05 g, 2.20 mmol) was added to a solution of HC≡CC_6H_4X-*p* (0.5 mmol) in methanol (20 cm^3), and the mixture was stirred until all the sodium was consumed. [Ru(16-TMC)-Cl_2]Cl (0.10 g, 0.20 mmol) and zinc amalgam were added, and this mixture was heated at reflux for 1 h to yield a yellow precipitate. After the system was cooled to room temperature, the resultant solid was collected and dissolved in a minimum amount of benzene. Slow diffusion of *n*-hexane into this solution afforded bright yellow crystals.

Complex **1** (X = OMe): yield 0.09 g, 67%. Anal. Calcd for $C_{34}H_{50}N_4O_2Ru$: C, 63.03; H, 7.78; N, 8.65. Found: C, 62.85; H, 7.92; N, 8.41. ^{1}H NMR (300 MHz, C_6D_6): δ 0.78, 0.83, 1.22−1.55 (m, 16H, CH_2), 2.41 (s, 12H, NCH_3), 3.40 (s, 6H, OCH_3), 4.02−4.14 (m, 8H, CH_2), 6.98 (d, 4H, $^3J_{HH}$ = 8.7 Hz, aryl H), 7.73 (d, 4H, $^3J_{HH}$ = 8.8 Hz, aryl H). $^{13}C\{^1H\}$ NMR (126 MHz, C_6D_6): δ 22.2, 22.6 (NCH_2CH_2), 50.0 (NCH_3), 55.0 (OCH_3), 60.7, 68.1 (NCH_2), 109.0 (C_β), 114.3, 126.1, 131.8 (aryl C), 156.2 (C_p), 158.7 (C_α). IR (cm^{-1}): ν(C≡C) 2002. FAB-MS: *m*/*z* 648 [M$^+$].

Complex **2** (X = Me): yield 0.08 g, 69%. Anal. Calcd for $C_{34}H_{50}N_4Ru$: C, 66.31; H, 8.18; N, 9.10. Found: C, 66.47; H, 8.18; N, 9.09. ^{1}H NMR (300 MHz, C_6D_6): δ 0.76, 0.81, 1.19−1.56 (m, 16H, CH_2), 2.24 (s, 6H, CH_3), 2.38 (s, 12 H, NCH_3), 3.96−4.23 (m, 8H, CH_2), 7.73 (d, 4H, $^3J_{HH}$ = 8.0 Hz, aryl H), 4 aryl H obscured by C_6D_6 solvent. $^{13}C\{^1H\}$ NMR (68 MHz, C_6D_6): δ 21.4 (CH_3), 22.1, 22.5, (NCH_2CH_2), 50.0 (NCH_3), 60.6, 68.0 (NCH_2), 110.0 (C_β), 129.1, 130.2, 131.0, 131.3, (aryl C), 161.2 (C_α). IR (cm^{-1}): ν(C≡C) 2003. FAB-MS: *m*/*z* 616 [M$^+$].

Complex **3** (X = H): yield 0.08 g, 68%. Anal. Calcd for $C_{32}H_{46}N_4Ru$: C, 65.39; H, 7.89; N, 9.53. Found: C, 65.07; H,

(10) Che, C. M.; Yam, V. W. W. *Adv. Inorg. Chem.* **1992**, *39*, 233.
(11) For example, see: (a) Touchard, D.; Haquette, P.; Daridor, A.; Romero, A.; Dixneuf, P. H. *Organometallics* **1998**, *17*, 3844. (b) Touchard, D.; Haquette, P.; Guesmi, S.; Le Pichon, L.; Daridor, A.; Toupet, L.; Dixneuf, P. H. *Organometallics* **1997**, *16*, 3640 and references therein. (c) Yi, C. S.; Liu, N.; Rheingold, A. L.; Liable-Sands, L. M. *Organometallics* **1997**, *16*, 3910. (d) Lee, H. M.; Yao, J.; Jia, G. *Organometallics* **1997**, *16*, 3927. (e) de los R'os, I.; Jiménez-Tenorio, M.; Puerta, M. C.; Valerga, P. *J. Am. Chem. Soc.* **1997**, *119*, 6529. (f) Ting, P. C.; Lin, Y. C.; Lee, G. H.; Cheng, M. C.; Wang, Y. *J. Am. Chem. Soc.* **1996**, *118*, 6433. (g) Albertin, G.; Antoniutti, S.; Bordignon, E.; Cazzaro, F.; Ianelli, S.; Pelizzi, G. *Organometallics* **1995**, *14*, 4114. (h) Esteruelas, M. A.; Lahoz, F. J.; López, A. M.; Oñate, E.; Oro, L. A. *Organometallics* **1994**, *13*, 1669. (i) Trost, B. M.; Flygare, J. A. *J. Am. Chem. Soc.* **1992**, *114*, 5476.
(12) (a) Slugovc, C.; Mereiter, K.; Schmid, R.; Kirchner, K. *J. Am. Chem. Soc.* **1998**, *120*, 6175. (b) Slugovc, C.; Mauthner, K.; Kacetl, M.; Mereiter, K.; Schmid, R.; Kirchner, K. *Chem. Eur. J.* **1998**, *4*, 2043. (c) Santos, A.; López, J.; Galán, A.; González, J. J.; Tinoco, P.; Echavarren, A. M. *Organometallics* **1997**, *16*, 3482. (d) Bianchini, C.; Innocenti, P.; Peruzzini, M.; Romerosa, A.; Zanobini, F. *Organometallics* **1996**, *15*, 272.
(13) Yang, S. M.; Chan, M. C. W.; Cheung, K. K.; Che, C. M.; Peng, S. M. *Organometallics* **1997**, *16*, 2819.
(14) Che, C. M.; Wong, K. Y.; Poon, C. K. *Inorg. Chem.* **1986**, *25*, 1809.
(15) Che, C. M.; Poon, C. K. *Pure Appl. Chem.* **1988**, *60*, 495.

Table 1. Crystal Data

	1	3	5
formula	$C_{34}H_{50}N_4O_2Ru$	$C_{32}H_{46}N_4Ru$	$C_{32}H_{44}N_4Cl_2Ru$
fw	647.87	587.81	656.70
cryst size, mm	0.35 × 0.10 × 0.07	0.30 × 0.15 × 0.10	0.30 × 0.20 × 0.10
cryst syst	triclinic	monoclinic	monoclinic
space group	$P\bar{1}$ (No. 2)	$P2_1/a$ (No. 14)	$P2_1/a$ (No. 14)
a, Å	8.399(2)	8.617(3)	8.460(2)
b, Å	9.670(2)	17.563(3)	16.975(2)
c, Å	10.292(2)	9.381(2)	10.904(2)
α, deg	89.12(2)		
β, deg	73.23(2)	91.96(2)	94.61(2)
γ, deg	88.85(2)		
V, Å^3	800.1(3)	1418.9(5)	1560.8(5)
Z	1	2	2
D_c, g cm^{-3}	1.344	1.376	1.397
μ, cm^{-1}	5.26	5.80	7.01
$F(000)$	342	620	684
$2\theta_{max}$, deg	51	46	51
no. of unique rflns	2761 (R_{int} = 0.031)	2104 (R_{int} = 0.017)	2831 (R_{int} = 0.055)
no. of obsd rflns	2676 ($I > 3\sigma(I)$)	1434 ($I > 3\sigma(I)$)	2037 ($I > 3\sigma(I)$)
no. of variables	187	169	178
R,[a] R_w[b]	0.037, 0.050	0.030, 0.035	0.039, 0.051
GOF[c]	1.75	2.03	1.73
residual peaks, e Å^{-3}	+0.47, −0.66,	+0.45, −0.29	+0.60, −0.55

[a] $R = \sum||F_o| - |F_c||/\sum|F_o|$. [b] $R_w = [\sum w(|F_o| - |F_c|)^2/\sum w|F_o|^2]^{1/2}$. [c] GOF = $[\sum w(|F_o| - |F_c|)^2/(n - p)]^{1/2}$.

7.70; N, 9.48. ^{1}H NMR (500 MHz, C_6D_6): δ 0.76, 0.79, 1.19−1.71 (m, 16H, CH_2), 2.36 (s, 12H, NCH_3), 3.94−4.05 (m, 8H, CH_2), 7.07 (t, 2H, $^3J_{HH}$ = 7.3 Hz, H_p), 7.33 (t, 4H, $^3J_{HH}$ = 7.6 Hz, H_m), 7.78 (d, 4H, $^3J_{HH}$ = 7.1 Hz, H_o). $^{13}C\{^1H\}$ NMR (126 MHz, C_6D_6): δ 22.4, 22.8, (NCH_2CH_2), 50.2 (NCH_3), 61.0, 68.4 (NCH_2), 110.0 (C_β), 122.8, 127.9, 131.5, 133.3, (aryl C), 163.5 (C_α). IR (cm^{-1}): ν(C≡C) 2012. FAB-MS: m/z 588 [M$^+$].

Complex **4** (X = F): yield 0.06 g, 48%. Anal. Calcd for $C_{32}H_{44}N_4F_2Ru$: C, 61.62; H, 7.11; N, 8.98. Found: C, 61.37; H, 6.97; N, 8.70. ^{1}H NMR (500 MHz, C_6D_6): δ 0.70−1.71 (m, 16H, CH_2), 2.33 (s, 12H, NCH_3), 3.91−3.99 (m, 8H, CH_2), 6.99, 7.53 (m, 8H, aryl H). $^{13}C\{^1H\}$ NMR (68 MHz, C_6D_6): δ 21.9, 22.3 (NCH_2CH_2), 49.2 (NCH_3), 61.0, 67.5 (NCH_2), 109.3 (C_β), 115.1 (d, J_{FC} = 21.8 Hz, aryl C), 132.0 (aryl C), 159.8 (d, $^1J_{FC}$ = 242 Hz, C_p), 161.2 (C_α). IR (cm^{-1}): ν(C≡C) 2006. FAB-MS: m/z 624 [M$^+$].

Complex **5** (X = Cl): yield 0.07 g, 53%. Anal. Calcd for $C_{32}H_{44}N_4Cl_2Ru$: C, 58.53; H, 6.75; N, 8.53. Found: C, 58.73; H, 6.94; N, 8.56. ^{1}H NMR (300 MHz, C_6D_6): δ 0.73−1.48 (m, 16H, CH_2), 2.28 (s, 12H, NCH_3), 3.79−3.93 (m, 8H, CH_2), 7.30 (d, 4H, $^3J_{HH}$ = 8.5 Hz, aryl H), 7.50 (d, 4H, $^3J_{HH}$ = 8.5 Hz, aryl H). $^{13}C\{^1H\}$ NMR (126 MHz, C_6D_6): δ 22.0, 22.4 (NCH_2CH_2), 49.8 (NCH_3), 60.6, 68.0 (NCH_2), 109.7 (C_β), 128.6, 131.0, 132.1 (aryl C), 165.5 (C_α). IR (cm^{-1}): ν(C≡C) 2004. FAB-MS: m/z 658 [M$^+$].

[Ru(16-TMC)(C≡CPh)(CO)]PF$_6$ (6). Oxygen gas was introduced into a 1,2-dichloroethane solution (15 cm^3) of **3** (0.10 g, 0.20 mmol) and NH_4PF_6 (0.16 g, 1.0 mmol) for 3 h, during which time the color of the solution changed from yellow to green and eventually to yellow with the appearance of a yellow precipitate. The solid was filtered, washed with cold water and diethyl ether, and air-dried. Recrystallization from CH_2Cl_2/diethyl ether yielded yellow crystals (yield 0.09 g, 68%). Anal. Calcd for $C_{25}H_{41}N_4ORuF_6P$: C, 45.52; H, 6.26; N, 8.49. Found: C, 45.42; H, 5.93; N, 8.30. ^{1}H NMR (300 MHz, CD_2Cl_2): δ 1.50−1.68, 1.93−2.11, 2.40−2.48, 3.18−3.38, 3.98−4.18 (m, 24H, CH_2), 2.65, 2.67 (two singlets, 12H, NCH_3), 7.12−7.13, 7.30−7.38 (m, 5H, C_6H_5). $^{13}C\{^1H\}$ NMR (68 MHz, CD_3CN): δ 21.5, 21.8 (NCH_2CH_2), 52.5 (NCH_3), 63.7, 71.9 (NCH_2), 126.6, 129.3, 130.0, 131.6, 136.4, 143.7 (aryl C, C_α, C_β), 202.8 (CO). IR (cm^{-1}): ν(C≡C) 2080 w, ν(C≡O) 1916 s. FAB-MS: m/z 515 [M$^+$].

X-ray Crystallography. Crystals of **1**, **3**, and **5** were obtained by diffusion of *n*-hexane into benzene solutions. Crystal data and details of collection and refinement are summarized in Table 1.

Diffraction experiments were performed at 301 K on MAR (**1** and **5**) and Enraf-Nonius CAD4 (**3**) diffractometers using graphite-monochromatized Mo Kα radiation (λ = 0.710 73 Å). The structures were solved by direct methods (**1** and **5**, SIR92[16]) and by Patterson methods (**3**, PATTY[17]), expanded by Fourier techniques and refined by full-matrix least squares using the TeXsan[18] program on a Silicon Graphics Indy computer. For **1**, a crystallographic asymmetric unit consists of a half-molecule with the Ru atom at the origin. All 21 non-H atoms were refined anisotropically, and 25 H atoms at calculated positions with thermal parameters equal to 1.3 times that of the attached C atoms were not refined. Atoms marked with asterisks have coordinates at $-x$, $-y$, $-z$. For **3**, a crystallographic asymmetric unit consists of a half-molecule with the Ru atom at the origin. All 19 non-H atoms were refined anisotropically, and 23 H atoms at calculated positions were not refined. Atoms marked with asterisks have coordinates at $-x$, $-y$, $-z$. For **5**, a crystallographic asymmetric unit consists of a half-molecule with the Ru atom at $^1/_2$, $^1/_2$, 0. All 20 non-H atoms were refined anisotropically, and 22 H atoms at calculated positions were not refined. Atoms marked with asterisks have coordinates at $1 - x$, $1 - y$, $-z$.

Results and Discussion

Synthesis and Characterization. Treatment of the conveniently prepared ruthenium(III) complex [Ru(16-TMC)Cl$_2$]Cl[14] with zinc amalgam, NaOMe, and alkyne afforded the desired Ru(II) *trans*-bis(*σ*-arylacetylide) derivatives as yellow crystalline solids (Scheme 1). Reduction of the Ru(III) precursor yields the [Ru^{II}(16-TMC)Cl$_2$] species, which is substitutionally labile and facilitates ligand exchange. Complexes **1**−**5** are stable for several days in the solid state and in deoxygenated solutions. Under aerobic conditions, solutions of **1**−**5** are unstable and a color change from yellow to green is detectable within 3 h (see Oxidation).

(16) SIR92: Altomare, A.; Cascarano, M.; Giacovazzo, C.; Guagliardi, A.; Burla, M. C.; Polidori, G.; Camalli, M. *J. Appl. Crystallogr.* **1994**, *27*, 435.

(17) PATTY: Beurskens, P. T.; Admiraal, G.; Beursken, G.; Bosman, W. P.; Garcia-Granda, S.; Gould, R. O.; Smits, J. M. M.; Smykalla, C. The DIRDIF Program System, Technical Report of the Crystallography Laboratory; University of Nijmegen, Nijmegen, The Netherlands, 1992.

(18) TeXsan: Crystal Structure Analysis Package; Molecular Structure Corp., The Woodlands, TX, 1985 and 1992.

Scheme 1

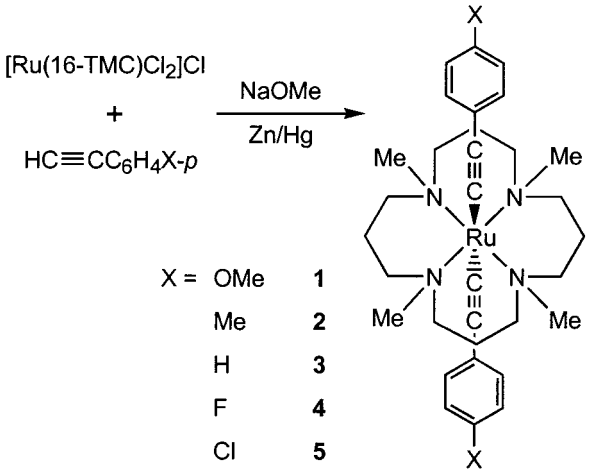

The bis(acetylide) complexes have been characterized by various spectroscopic techniques. The IR spectra of **1**−**5** are comparable, with an intense band for the asymmetric C≡C stretch, ν_{as}(C≡C) at 2002−2012 cm^{-1}. These values are among the lowest reported for ruthenium acetylide derivatives.[2] For example, the ν_{as}(C≡C) value for *trans*-[Ru(16-TMC)(C≡CPh)$_2$] (**3**) is 2012 cm^{-1} (KBr), which is lower than in related complexes with phosphine auxiliary ligands, such as *trans*-[Ru(C≡CPh)$_2$(PEt$_3$)$_2$(CO)$_2$] (2093 cm^{-1} in CH_2Cl_2)[19] and *trans*-[Ru(C≡CPh)$_2$(depe)$_2$] (2054 cm^{-1} in CH_2Cl_2, depe = $Et_2PCH_2CH_2PEt_2$).[20] The FT Raman spectrum of complex **3** shows an intense symmetric C≡C stretch at 2033 cm^{-1}, which again is distinctly lower than that for *trans*-[Ru(C≡CPh)$_2$(PEt$_3$)$_2$(CO)$_2$] (2101 cm^{-1}).[21] In the $^{13}C\{^1H\}$ NMR spectra of complexes **1**−**5**, a singlet is observed at 158.7−165.5 ppm (C_6D_6) for the α-acetylide carbon. This resonance for **3** at 163.5 ppm is significantly downfield from that for the phosphine analogues *trans*-[Ru(C≡CPh)$_2$(depe)$_2$] (130.6 ppm in C_6D_6)[22] and *trans*-[Ru(C≡CPh)$_2$(PMe$_3$)$_4$] (132.5 ppm in CD_2Cl_2).[23] In contrast, the signals for the *β*-acetylide carbons in these complexes are similar (111.0, 112.8, and 108.2 ppm, respectively). The low ν_{as}(C≡C) and ν_s(C≡C) stretching frequencies and the downfield shifts of C_α in **1**−**5**, relative to derivatives with phosphine donors, are consistent with the greater *σ*-donating ability of the tertiary amine ligand 16-TMC. This in turn promotes increased metal-to-acetylide *π* back-bonding from the electron-rich Ru(II) center.

The UV−vis absorption data of the bis(arylacetylide) complexes are summarized in Table 2. The absorption spectrum of **2** is shown in Figure 1. The absorption spectra of **1**−**5** in CH_2Cl_2 contain a high-energy band (λ_{max} 248−255 nm) and an intense band with λ_{max} in the 379−408 nm region ($\epsilon_{max} > 10^4$ dm^3 mol^{-1} cm^{-1}). We assign the latter absorption to a d_π(Ru) → *π**(CCAr) metal-to-ligand charge transfer (MLCT) transition. It is apparent that the MLCT transition red-shifts in energy as the electron-withdrawing ability of the *para* substituents on the arylacetylide groups increases. Hence, an electron-withdrawing substituent stabilizes the *π**(CCAr) orbital and lowers the energy of the MLCT transition. The exception in this regard is complex **4**, where the large resonance effect of the fluoride group can destabilize *π**(CCAr) and increase the MLCT energy. We note that the Ru(II) → *π**(py) MLCT transition of *cis*-[Ru([14]aneN$_4$)(py)$_2$]$^{2+}$, bearing a macrocyclic tetradentate amine ligand, occurs at 378 nm (H_2O).[24] This is comparable in energy to the MLCT transitions of complexes **1**−**5**, despite electronic differences between the pyridine group and the anionic arylacetylide moieties. Furthermore, the Ru(II) → *π**(py) MLCT transition of *cis*-[Ru(NH$_3$)$_5$(py)]$^{2+}$ appears at 407 nm (CH_3CN).[25]

Table 2. UV−Visible Absorption Data for [Ru(16-TMC)(C≡CC$_6$H$_4$X-*p*)$_2$] (1−5) and 6

	λ_{max}, nm (log ϵ)	
complex	CH_2Cl_2	CH_2Cl_2 + Ce(IV)/MeOH[a]
1 (X = OMe)	248 (4.54), 379 (4.52)	675 (sh), 768
2 (X = Me)	250 (4.64), 392 (4.57)	648 (sh), 730
3 (X = H)	250 (4.46), 394 (4.48)	646 (sh), 729
4 (X = F)	246 (4.48) 388 (4.45)	633 (sh), 716
5 (X = Cl)	255 (4.55), 408 (4.58)	638 (sh), 722
6	256 (4.10), 271 (3.97, sh)	

[a] Vibronic bands. See Figure 6 for full spectrum of **1**$^+$.

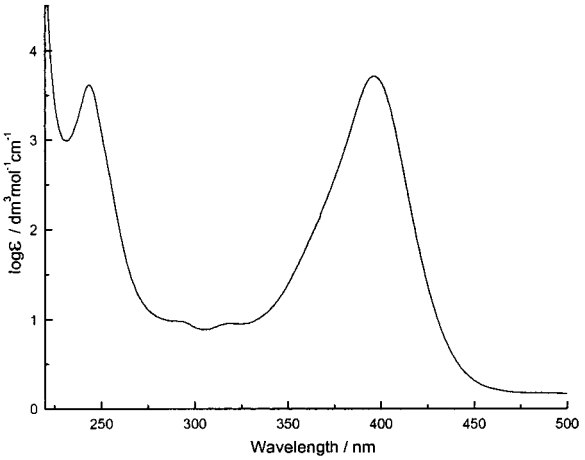

Figure 1. UV−vis absorption spectrum of **2** in CH_2Cl_2 at room temperature.

Crystal Structures. Figures 2 and 3 show perspective views of complexes **1** and **5**, respectively (for **3**, see the Supporting Information). Selected bond distances and angles are listed in Table 3.

The ruthenium atom in each structure resides in an octahedral environment and is coordinated by four equatorial nitrogen atoms of 16-TMC and two *σ*-arylacetylide ligands in a *trans* arrangement. The six-membered chelate rings of the Ru(16-TMC) fragment are all in chair forms, with the *N*-methyl groups adopting the "two up, two down" configuration as in *trans*-[Ru(16-TMC)O$_2$]$^{2+}$.[26] The Ru−C (**1**, 2.077(3) Å; **3**, 2.077(4) Å; **5**, 2.073(4) Å) and C≡C (**1**, 1.195(4) Å; **3**,

(19) Sun, Y.; Taylor, N. J.; Carty, A. J. *J. Organomet. Chem.* **1992**, *423*, C43.
(20) Atherton, Z.; Faulkner, C. W.; Ingham, S. L.; Kakkar, A. K.; Khan, M. S.; Lewis, J.; Long, N. J.; Raithby, P. R. *J. Organomet. Chem.* **1993**, *462*, 265.
(21) Sun, Y.; Taylor, N. J.; Carty, A. J. *Organometallics* **1992**, *11*, 4293.
(22) Field, L. D.; George, A. V.; Hockless, D. C. R.; Purches, G. R.; White, A. H. *J. Chem. Soc., Dalton Trans.* **1996**, 2011.
(23) Rappert, T.; Yamamoto, A. *Organometallics* **1994**, *13*, 4984.
(24) Che, C. M.; Kwong, S. S.; Poon, C. K.; Lai, T. F.; Mak, T. C. W. *Inorg. Chem.* **1985**, *24*, 1359.
(25) Creutz, C.; Chou, M. H. *Inorg. Chem.* **1987**, *26*, 2995.
(26) Mak, T. C. W.; Che, C. M.; Wong, K. Y. *J. Chem. Soc., Chem. Commun.* **1985**, 986.

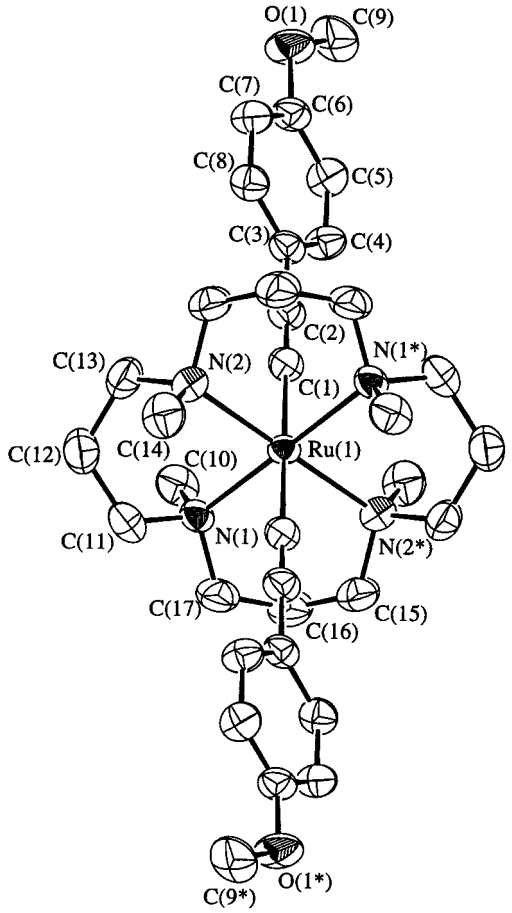

Figure 2. Perspective view of *trans*-[Ru(16-TMC)(C≡CC_6H_4OMe-*p*)$_2$] (**1**) (50% probability ellipsoids, hydrogen atoms omitted for clarity).

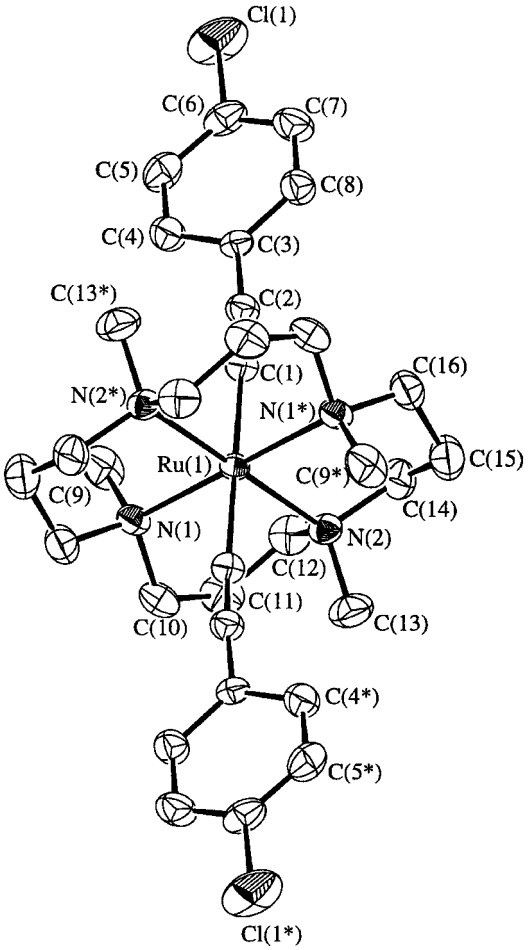

Figure 3. Perspective view of *trans*-[Ru(16-TMC)(C≡CC_6H_4Cl-*p*)$_2$] (**5**) (50% probability ellipsoids, hydrogen atoms omitted for clarity).

1.198(6) Å; **5**, 1.190(5) Å) bond lengths in this work are typical for ruthenium(II) bis(acetylide) complexes.[1,2] The latter distances are evidently insensitive to the nature of the *para* substituent. By comparison, the C≡C distances in *trans*-[Ru(C≡CPh)$_2$(dppe)$_2$] are 1.194(7) and 1.207(7) Å,[20] while that in *trans*-[Ru(C≡CPh)$_2$(PEt_3)$_2$-$(CO)_2$] is 1.200(4) Å.[19] The virtual linearity of the Ar−C≡C−Ru−C≡C−Ar fragment is maintained in these structures. For example, the Ru−C(1)−C(2) and C(1)−C(2)−C(3) angles in complex **1** are 175.9(3) and 174.9-(3)°, respectively.

Electrochemistry. Cyclic voltammetry was used to examine the electrochemistry of the bis(*σ*-arylacetylide) complexes (Table 4). The cyclic voltammograms of complexes **1**−**5** reveal two quasi-reversible oxidation couples at $E_{1/2} = -0.83$ to -0.68 V and $E_{1/2} = +0.54$ to $+0.80$ V vs $Cp_2Fe^{0/+}$ (Figure 4 for **2**). For complex **2**, ΔE_p and the $E_{p,a}/E_{p,c}$ ratio of the first couple approaches 0.07 V and 0.90, respectively, and a one-electron process was established by constant-potential electrolysis. We assign this couple to $Ru^{III/II}$, and the half-reaction is

$$[Ru^{III}(16\text{-TMC})(C{\equiv}CAr)_2]^+ + e^- \rightarrow [Ru^{II}(16\text{-TMC})(C{\equiv}CAr)_2] \quad (1)$$

The variation of the $E_{1/2}(Ru^{III/II})$ values for **1**−**5** corresponds to a red shift of the MLCT transition (except for **4**; see the discussion on absorption data). Changing the substituents on the acetylide groups is expected to influence the π^* orbital and hence the MLCT energy. Similarly, if there is a *significant* $d_\pi(Ru) \rightarrow \pi^*(CCAr)$ back-bonding interaction in the *trans*-[Ru(C≡CAr)$_2$] moiety, the Ru(II) electron density and hence the $E°(Ru^{III/II})$ value would also be affected by the energy of the $\pi^*(CCAr)$ orbital. It is interesting to note that the $E_{1/2}(Ru^{III/II})$ value of *trans*-[Ru(16-TMC)Cl_2]$^+$ (−0.60 V vs $Cp_2Fe^{0/+}$)[14] is partially higher than those for **1**−**5**. In terms of *σ*-donor strength, ArC≡C$^-$ is superior to Cl$^-$ for the stabilization of Ru(III) species because of the covalency of the Ru^{III}−CCAr bond. Nevertheless, the

Table 3. Selected Bond Distances (Å) and Angles (deg)

[Ru(16-TMC)(C≡CC_6H_4OMe-*p*)$_2$] (**1**)			
Ru−N(1)	2.271(2)	Ru−C(1)	2.077(3)
Ru−N(2)	2.275(3)	C(1)−C(2)	1.195(4)
N(1)−C(17)	1.486(4)	C(2)−C(3)	1.439(4)
N(1)−Ru−N(2)	89.3(1)	N(1)−Ru−N(1*)	180.0
N(1)−Ru−N(2*)	90.7(1)	Ru−C(1)−C(2)	175.9(3)
N(1)−Ru−C(1)	92.2(1)	C(1)−C(2)−C(3)	174.9(3)
N(1)−Ru−C(1*)	87.8(1)		
[Ru(16-TMC)(C≡CC_6H_4Cl-*p*)$_2$] (**5**)			
Ru−N(1)	2.273(3)	Ru−C(1)	2.073(4)
Ru−N(2)	2.274(3)	C(1)−C(2)	1.190(5)
N(1)−C(10)	1.492(6)	C(2)−C(3)	1.440(5)
N(1)−Ru−N(2)	89.2(1)	N(1)−Ru−N(1*)	180.0
N(1)−Ru−N(2*)	90.8(1)	Ru−C(1)−C(2)	177.4(4)
N(1)−Ru−C(1)	91.1(1)	C(1)−C(2)−C(3)	174.2(4)
N(1)−Ru−C(1*)	88.9(1)		

Table 4. Electrochemical Data for [Ru(16-TMC)(C≡CC$_6$H$_4$X-*p*)$_2$]^a

complex	$E_{1/2}$(Ru$^{IV/III}$)	$E_{1/2}$(Ru$^{III/II}$)
1 (X = OMe)	+0.54	−0.83
2 (X = Me)	+0.70	−0.80
3 (X = H)	+0.76	−0.74
4 (X = F)	+0.76	−0.72
5 (X = Cl)	+0.80	−0.68

^{a} $E_{1/2}$ (V vs $Cp_2Fe^{0/+}$, scan rate 100 mV/s) in CH_2Cl_2 at 298 K with 0.1 M $NBu^n_4PF_6$ as supporting electrolyte.

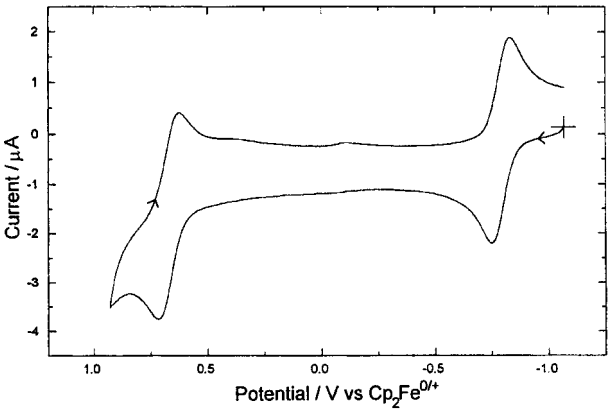

Figure 4. Cyclic voltammogram of **2** vs $Cp_2Fe^{0/+}$ in CH_2Cl_2 at room temperature.

former is also a better π-acceptor than Cl^- and can accommodate Ru^{II} ions through increased π back-bonding interactions.

The *trans*-[Ru^{III}(16-TMC)(C≡CAr)$_2$]$^+$ species can be generated by electrolysis of the Ru(II) precursors **1**−**5** using thin-layer spectroelectrochemistry. Figure 5 depicts the spectral changes associated with the electrochemical oxidation of **5** at −0.47 V (the initial trace shows that partial oxidation has occurred under the reaction conditions). Isosbestic spectral changes are recorded: the MLCT absorption band disappears and is replaced by a new band at λ_{max} 722 nm. As discussed in the following section, this low-energy band is assigned to a p_π(ArCC) → d_{π^*}(Ru^{III}) LMCT transition.

The second couple (+0.54 V for **1**, +0.70 to +0.80 V for **2**−**5**) is less reversible, especially with slower scan rates (<100 mV s^{-1}). Because the peak currents for the first and second couples are similar, we infer that the latter also originates from a one-electron oxidation, namely Ru$^{IV/III}$:

$$[Ru^{IV}(16\text{-TMC})(C{\equiv}CAr)_2]^{2+} + e^- \rightarrow [Ru^{III}(16\text{-TMC})(C{\equiv}CAr)_2]^{+} \quad (2)$$

This assignment is supported by the fact that the $E_{1/2}$ values for complexes **2**−**5** are comparable, despite varying the phenyl *para* substituents (CH_3, H, F, and Cl). The 16-TMC ligand is known to be electrochemically inactive upon coordination to a metal ion.[15] The noticeably lower $E_{1/2}$(Ru$^{IV/III}$) value for complex **1** can be rationalized by the mesomeric effect of the methoxy substituent in the electrochemically generated [Ru^{IV}(16-TMC)(C≡CC$_6$H$_4$OMe-*p*)$_2$]$^{2+}$ species, where π-bonding between Ru^{IV} and the acetylide group is stabilized by electron donation from the OMe moiety. The $E_{1/2}$(Ru$^{IV/III}$) values for **1**−**5** are significantly lower than that for *trans*-[Ru(16-TMC)Cl$_2$]$^{2+}$ (1.16 V vs $Cp_2Fe^{0/+}$).[14] This

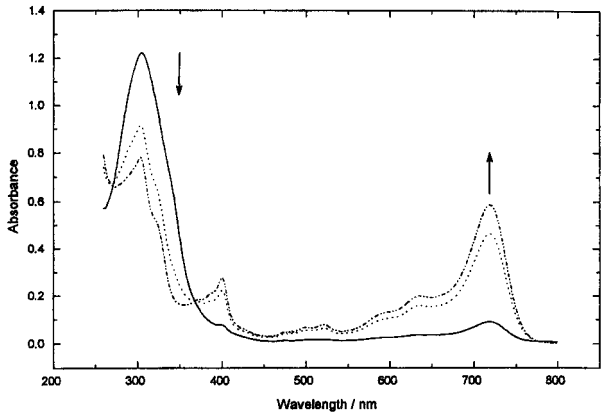

Figure 5. UV−vis spectral changes during electrochemical oxidation (at −0.47 V vs $Cp_2Fe^{0/+}$) of **5** in 0.1 M $NBu^n_4PF_6$/CH_2Cl_2 solution: (—) initial trace; (···) trace after 10 min; (—··—) trace after 50 min.

implies that, for ruthenium(IV) species, ArC≡C$^-$ is a better donor than Cl^- and metal−ligand π-bonding interactions are presumably more prevalent for the former. The electrochemical data also demonstrate the merit of macrocyclic tertiary amine ligands for the kinetic stabilization of highly oxidizing metal acetylide complexes. In this study, the 16-TMC ligand may also provide steric protection for the [Ru(C≡CAr)$_2$] moiety from nucleophilic attack.

Oxidation. Introduction of dioxygen into a 1,2-dichloroethane solution of **3** containing NH_4PF_6 afforded [Ru(16-TMC)(C≡CC$_6$H$_5$)(CO)]PF$_6$ (**6**). Transformation of an acetylide to a carbonyl ligand by oxidative cleavage has precedent.[13,27] The mass spectrum of **6** reveals a cluster at *m*/*z* 515 which corresponds to the parent cation. A low-field singlet at 202.8 ppm in the ^{13}C NMR spectrum and a strong IR absorption at 1916 cm^{-1} are characteristic of a terminal carbonyl ligand.

The complexes **1**−**5** can be chemically oxidized to [Ru^{III}(16-TMC)(C≡CAr)$_2$]$^+$. Addition of methanolic $(NH_4)_2Ce(NO_3)_6$ to a dichloromethane solution of **1**−**5** caused an immediate color change from yellow to green. As shown in Figure 6, the UV−vis spectrum of *trans*-[Ru^{III}(16-TMC)(C≡CC$_6$H$_4$OMe-*p*)$_2$]$^+$ (**1**$^+$) obtained by Ce(IV) oxidation closely resembles that by electrochemical oxidation of **5** (Figure 5). Intense vibronically structured absorptions with λ_{max} varying from 716 to 768 nm are observed for **1**−**5**, with vibrational progressions in the range 1730−1830 cm^{-1} (Table 2). These values are lower than the ground-state ν(C≡C) value but are consistent with reduced C≡C stretching frequencies associated with an acetylide-to-Ru(III) charge transfer excited state. We therefore tentatively assign these bands to a p_π(ArCC) → d_{π^*}(Ru^{III}) ligand-to-metal charge transfer (LMCT) transition. It is pertinent to compare these absorptions with the LMCT transition energies of *trans*-[Ru(14-TMC)(NCS)$_2$]$^+$ (λ_{max} 594 nm in H_2O),[28] *trans*-[Ru([14]aneN$_4$)I$_2$]$^+$ (λ_{max} 601 nm in DMSO),[29] and *trans*-[Ru(en)$_2$I$_2$]$^+$ (λ_{max} 573 nm in MeOH, en = 1,2-diamino-

(27) (a) Oro, L. A.; Ciriano, M. A.; Campo, M.; Foces-Foces, C.; Cano, F. H. *J. Organomet. Chem.* **1985**, *289*, 117. (b) Bruce, M. I.; Swincer, A. G.; Wallis, R. C. *J. Organomet. Chem.* **1979**, *171*, C5.

(28) Che, C. M.; Kwong, S. S.; Poon, C. K. *Inorg. Chem.* **1985**, *24*, 1601.

(29) Poon, C. K.; Che, C. M. *Inorg. Chem.* **1981**, *20*, 1640.

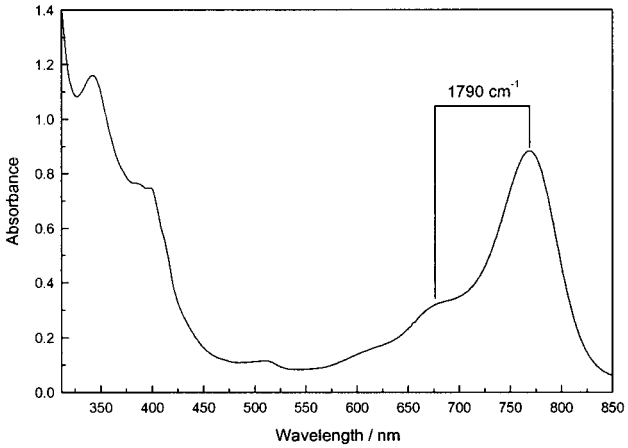

Figure 6. UV−vis absorption spectrum of **1** in CH_2Cl_2 after addition of methanolic $(NH_4)_2Ce(NO_3)_6$ at room temperature.

ethane).[30] Since the natures of the ancillary amine ligands are similar, these data suggest that the optical electronegativity of the p_π electrons in $ArC{\equiv}C^-$ is comparable to those in NCS^- and I^-. Attempts to isolate the *trans*-$[Ru^{III}(16\text{-TMC})(C{\equiv}CAr)_2]^+$ complexes were unsuccessful, presumably because the +3 oxidation state in this system readily transforms to other Ru(II) species. For example, we have identified the Ru(II) carbonyl complex **6** as one of the products in the oxidation of the phenyl derivative **3**.

Conclusion. *trans*-Bis(acetylide)metal complexes have potential applications as linear rigid-rod motifs in material chemistry and electronic communication. In this work, a systematic series of ruthenium(II) bis(*σ*-arylacetylide) complexes supported by 16-TMC has been synthesized from $[Ru^{III}(16\text{-TMC})Cl_2]Cl$. Trends in spectroscopic, structural, and electrochemical data have been examined. Low $\nu(C{\equiv}C)$ stretches are observed in the IR spectra, while the cyclic voltammograms of the bis(acetylide) derivatives reveal two quasi-reversible oxidation couples, namely $Ru^{III/II}$ and $Ru^{IV/III}$. The role of the tertiary amine ligand 16-TMC is apparent: its strong *σ*-donating strength is manifested in substantial metal-to-acetylide π back-bonding, while its ability to kinetically stabilize highly oxidized species, in this case $[Ru^{IV}(C{\equiv}CAr)_2]^{2+}$, is exemplified. Oxidation of the Ru(II) acetylide complexes by Ce(IV) or by electrochemical means yielded low-energy vibronic UV−vis absorption bands, which are tentatively assigned as $p_\pi(ArCC) \rightarrow d_{\pi^*}(Ru^{III})$ LMCT transitions.

Acknowledgment. We thank the University of Hong Kong (for a postgraduate studentship to M.-Y.C.) and the Hong Kong Research Grants Council for support. We are grateful to Dr. V. M. Miskowski for helpful discussions.

Supporting Information Available: A figure giving the ORTEP plot of **3** and tables of crystal data, atomic coordinates, calculated hydrogen coordinates, anisotropic displacement parameters, and bond distances and angles for **1**, **3**, and **5**. This material is available free of charge via the Internet at http://pubs.acs.org.

OM990009D

(30) Poon, C. K.; Che, C. M. *J. Chem. Soc., Dalton Trans.* **1980**, 756.